Authors

Tyko Shoji, Wanyan Xie, Kevin Silverman, Ari Feldman, Todd Harvey, Richard Mirin, and Thomas Schibli

Optica

Ultra-low-noise monolithic mode-locked solid-state laser

Tyko D. Shoji,[1] Wanyan Xie,[1] Kevin L. Silverman,[2] Ari Feldman,[2] Todd Harvey,[2] Richard P. Mirin,[2] and Thomas R. Schibli[1,3,*]

[1]Department of Physics, University of Colorado, Boulder, Colorado 80309-0390, USA
[2]National Institute of Standards and Technology, 325 Broadway, Boulder, Colorado 80305, USA
[3]JILA, NIST, and the University of Colorado, Boulder, Colorado 80309-0440, USA
*Corresponding author: trs@colorado.edu

Low-noise, high-repetition-rate mode-locked solid-state lasers are attractive for precision measurement and microwave generation, but the best lasers in terms of noise performance still consist of complex, bulky optical setups, which limits their range of applications. In this Letter, we present an approach for producing highly stable pulse trains with a record-low residual integrated offset frequency phase noise of 14 mrad at 1 GHz fundamental repetition rate using a monolithic mode-locked solid-state laser. The compact monolithic design simplifies implementation of the laser by fixing the cavity parameters and operates using just 265 mW of 980 nm pump light. © 2016 Optical Society of America

OCIS codes: (140.4050) Mode-locked lasers; (140.3580) Lasers, solid-state; (140.7090) Ultrafast lasers.

http://dx.doi.org/10.1364/OPTICA.3.000995

Growing demands in fields such as optical communication and microwave photonics for ultra-low-noise femtosecond pulse trains at high fundamental repetition rates have led to impressive advances in oscillator design. Most notably, practical fiber oscillators with attosecond timing jitter and stabilized fiber combs with milliradians of residual phase noise in the optical domain were recently demonstrated [1–3]. Ideally, compact, robust mode-locked lasers could be operated at gigahertz-order pulse repetition rates to take full advantage of the greater power per mode for high signal-to-noise ratio beat notes and low timing jitter for precision measurements outside of the lab. However, attaining repetition rates greater than a few hundred megahertz has been a challenge for these lasers due to design constraints. The timing jitter of femtosecond lasers has a quadratic dependence on the fundamental pulse repetition rate, which makes repetition-rate scaling unfavorable from a noise perspective [4].

The combination of high repetition rate, short pulse durations, and low noise is desirable for applications such as high bit rate optical communication, optical sampling techniques, and microwave generation. Recent advances in low-noise microwave generation based on optical frequency division (OFD) have led to dramatic improvements in phase-noise performance [5–9]. The ultimate noise performance of an OFD system is limited by the stability of the optical reference at low offset frequencies, the flicker floor of the photodetector at medium offset frequencies, and the available RF power from the photodiode and the RF circuit thermal noise floor at high frequencies [10,11]. In practice, OFD systems are limited by the available output power and shot noise, inaccuracies in the interleavers to circumvent photodiode saturation [11], and by both fundamental and technical noise from the pulsed lasers [12].

The earliest optical frequency combs were exclusively produced by solid-state mode-locked lasers (MLLs), but now most of these lasers have been replaced by the easier-to-operate mode-locked fiber lasers. There have been a number of reports on monolithic mode-locked waveguide [13–16] and semiconductor lasers [17–20], as well as microresonator-based Kerr-frequency combs [21–25]. Such compact devices hold great promise to revolutionize the field of precision metrology yet again. However, all of these approaches are ultimately limited by the physics that governs their dynamics. If one requires the ultimate noise performance, then even some of the Ti:sapphire laser demonstrations in the 1990s easily outperform the most sophisticated, cryogenically stabilized microresonator-based setups. The reason lies in a combination of favorable features found in solid-state MLLs: a large number of photons per pulse, near-zero dispersion and self-phase modulation, low round-trip losses, and large optical mode volumes. By taking full advantage of these properties, the noise factors that arise from amplified spontaneous emission (i.e., coupling of vacuum fluctuations to the laser light), Gordon–Haus jitter, and thermo-refractive effects can be made negligible, leading to lower phase noise [4]. This is especially important when high repetition rates are desired (see Section 1 in Supplement 1). At this time, it still is possible to design low-noise solid-state lasers that outperform any other laser technology available. The challenge lies in the complexity required to achieve this ultimate performance in traditional solid-state MLLs. This has been the motivation for developing an alternative setup that is simple to use and implement without compromising low-noise performance and reliability.

Development of single-frequency and Q-switched, chip-scale solid-state lasers has progressed much further than their mode-locked counterparts. For instance, one can now buy ultra-compact, frequency-doubled chip-scale lasers as green laser pointers, or more sophisticated systems, such as the very successful non-planar ring oscillator (NPRO) design [26], which is still found in many research labs. However, femtosecond-mode-locking such lasers has proven difficult. Over the past decade, many groups have designed waveguide-based mode-locked laser designs that suffer from the same design problems that limit the performance of fiber, waveguide, and diode lasers, such as small mode volumes and limited peak power. In this Letter, we present the first phase-stabilized, fully monolithic solid-state oscillator. The projected pulse timing-jitter phase-noise power spectral density is below the detection floor of commercial microwave phase-noise analyzers (see Section 1 in Supplement 1). The robust, compact cavity is a promising design for new applications outside of the controlled lab environment.

The laser setup is shown in Fig. 1. A ~8.5 cm long CaF_2 spacer serves as the laser cavity. The laser mode inside the material is ~2 mm in diameter, except in the proximity of the laser glass. This ensures low nonlinearity and negligible thermo-refractive effects. CaF_2 has both excellent transparency at the laser wavelength as well as zero second-order dispersion around 1545 nm, which is very close to the center of the laser operation. Therefore, third-order dispersion compensation is the main requirement for short-pulse operation. This is accomplished by a Gires–Tournois interferometer (GTI) coating [27] that was directly deposited on the CaF_2 spacer. A semiconductor saturable absorber mirror (SESAM) [28] was directly affixed to the laser glass to initiate and sustain mode locking. It was based on a single, erbium-doped, low-temperature-grown InGaAs quantum well on an AlGaAs/GaAs Bragg stack, similar to the as-grown device reported by Lee et al. [29], but without the n-doping of the top layer. The SESAM had a saturable loss of ~0.5% and even less nonsaturable loss. No degradation of the SESAM was observed over several months of operation, demonstrating the excellent

stability of the InGaAs quantum well even at gigahertz repetition rates.

One of the biggest challenges for glass-based laser materials is their low thermal conductivity. This makes glass lasers prone to thermally induced mode distortions and can lead to power limitations. In this monolithic setup, the laser glass was cooled via the internal contact between the glass and the CaF_2 spacer [Fig. 2(b)]. This has proven to be a much more efficient cooling scheme than the typical side-cooling approach [Fig. 2(a)]. No thermal power limitations or associated mode distortions were observed even when pumping at levels 2–3 times higher than required for the mode-locked operation shown in Fig. 3. In continuous wave operation (i.e., without the SESAM), intracavity powers in excess of 100 W have been achieved without any measurable mode distortions or efficiency roll-off. In the work presented in this Letter, the laser was operated at room temperature without any external sources of cooling. The total heat load was less than 0.2 W.

Figures 3(a) and 3(b) show the performance of the laser when pumped with ~265 mW optical power at 977 nm from a single-mode, butterfly packaged pump diode stabilized with a polarization-maintaining fiber Bragg grating. The monolithic laser self-started into a stable mode-locking regime and emitted ~65 mW average output power through a 0.27% output coupler into a fundamental Gaussian beam mode with virtually no astigmatism. The coupling efficiency into a single-mode fiber (SMF) was over 90%. This is very close to the theoretical coupling limit of 92% for an uncoated fiber, indicating that the M^2 value of the beam was close to 1. An intracavity average power of 24 W was achieved by keeping the cavity round-trip losses below 0.7%. The RMS fluctuations in the output power were <0.03%, measured at a 1.67 s gate time over 140 min of unstabilized operation in air (see Fig. S1 in Supplement 1). The unstabilized relative intensity noise (RIN) spectrum is shown in the inset of Fig. 3(b) and meets the metrics required for low-noise OFD.

Most OFD schemes that yield ultra-low phase noise at low offset frequencies require either detection or active stabilization of the offset frequency (f_{ceo}) of the femtosecond oscillator. To phase-stabilize the offset frequency of this oscillator, ~30 mW average power was coupled into an all polarization-maintaining (PM)-fiber parabolic amplifier, yielding an average power of 630 mW and 62 fs pulses [Fig. 3(c)]. Approximately 97% of
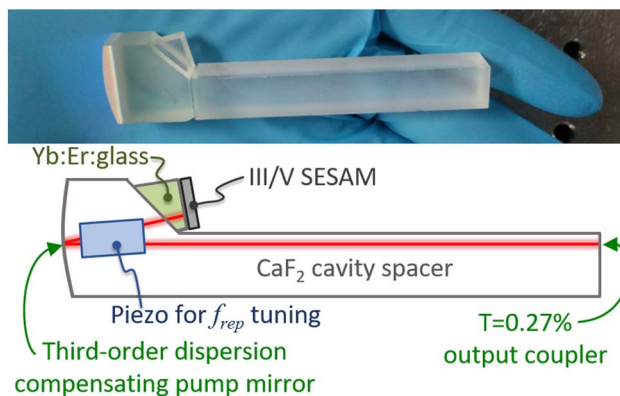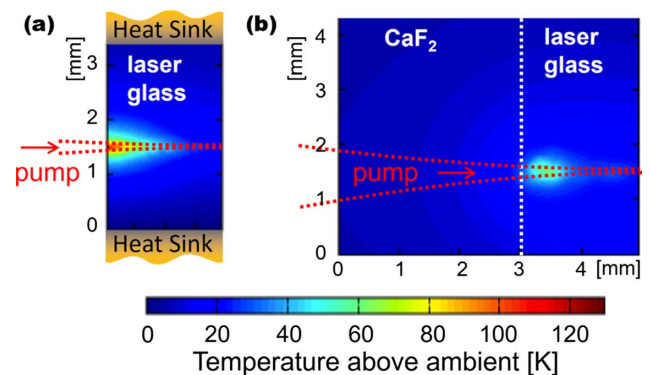

Fig. 1. Assembled cavity for size (top). The two CaF_2 pieces and the laser glass are joined permanently by chemically activated bonding or temporarily by an appropriate index-matching oil. The SESAM (semiconductor saturable absorber mirror) was attached via index-matching oil but could also be affixed via more permanent bonding techniques. The mirror coatings, including a third-order dispersion compensating mirror, were directly deposited on the CaF_2 spacer. The angle between the glass and the CaF_2 ensured linear polarization of the laser light.

Fig. 2. Calculated temperature distribution in the laser glass under 500 mW pumping at 977 nm. (a) Traditional method: side-cooled laser glass. (b) Laser glass heat-sunk through the CaF_2 cavity spacer. The CaF_2 heat sink dramatically lowers the laser glass surface temperature from 117 K above ambient for side-cooled glass to only 32 K above ambient when cooled through the CaF_2 spacer.
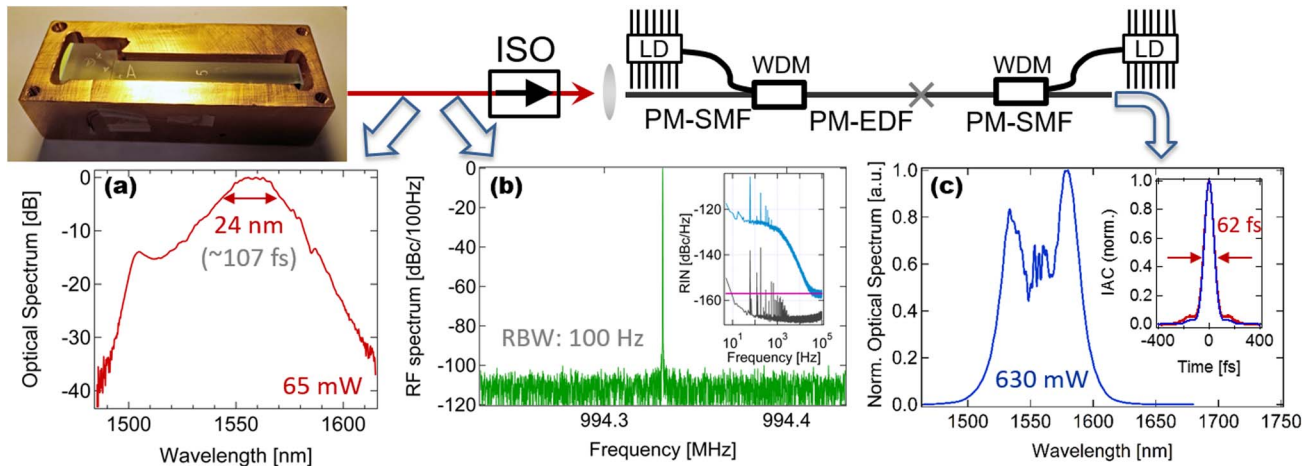
Fig. 3. (Top) Experimental setup of the fiber amplifier. ISO, isolator; LD, laser diode; WDM, wavelength division multiplexer; PM-SMF, polarization maintaining single-mode fiber; PM-EDF, polarization maintaining erbium-doped fiber. (a) Optical spectrum directly from the monolithic laser, showing a 24 nm FWHM bandwidth (~107 fs Fourier limit) at 65 mW average power. (b) RF spectrum around the fundamental repetition rate measured at 100 Hz resolution bandwidth (RBW), showing no relaxation oscillation-related noise peaks. Inset: measured RIN spectrum of the unstabilized laser (cyan) with an integrated (10 Hz–100 kHz) RMS RIN noise of <23 ppm, electronics noise floor (gray), and calculated shot-noise floor (purple). (c) Optical spectrum after parabolic amplification to 630 mW average power. Inset: measured intensity autocorrelation (red) and Fourier transform limit calculated from the optical spectrum (blue).

the pulse energy was in the center lobe of the pulse. A polarization-maintaining highly nonlinear fiber (PM-HNLF) spliced directly to the output of the parabolic amplifier led to an octave-spanning spectrum with ~535 mW average power. The octave-wide spectrum was then coupled to a frequency-doubling periodically poled lithium niobate (PPLN) crystal to create the f_{ceo} beat note at 1050 nm wavelength. The beat note showed an excellent contrast of ~110 dBc/Hz [Fig. 4(a)]. From soliton theory and the nonlinear phase shift determined from the f_{ceo} sidebands shown in Fig. 4(a), the net group delay dispersion of the cavity was determined to be ~30 fs^2. The net third-order dispersion was ~2000 fs^3. The free-running f_{ceo} RMS jitter remained within 10 kHz when measured at a 1 s gate time over several 1 h intervals [Fig. 4(b)], which, to our knowledge, is better than any previously reported result.

When locked to an RF reference via a simple low-delay PID controller that controlled the pump power of the laser, an integrated (100 Hz–1 MHz) residual RMS phase noise of 36 mrad at 1050 nm wavelength was achieved. By using an additional servo to remove some of the RIN of the pump diode, this value was further reduced to 14 mrad over the same frequency band (Fig. 4(c)), which, to the best of our knowledge, is the lowest residual phase-noise value reported to date for a 1 GHz oscillator. Even with an offset frequency of ~100 kHz at the peak of the servo bump (Fig. 4(c)), the contribution of the f_{ceo} residual noise to the phase noise of a 10 GHz microwave carrier would be as low as −180 dBc/Hz.

At low offset frequencies (<1 kHz), the residual noise was limited by the synthesizer (HP 8660B), which was used to generate the 465 MHz carrier to which the offset frequency was stabilized. At medium offset frequencies (~100 kHz), the residual noise was dominated by the "servo bump," and at high offset frequencies (>1 MHz), by light noise. Completely unstabilized, the offset frequency showed an intrinsic fast line width of ~200 Hz [Fig. 4(a), phase noise of −105 dBc/Hz at 1 MHz offset], and remained within ±0.5% of its average value over

a couple of weeks without thermal stabilization. With the pump-RIN servo on, the free-running fast f_{ceo} line width dropped below 50 Hz (see Section 2 in Supplement 1).

The large locking bandwidth demonstrated in Fig. 4(c) was possible despite the very slow response (~1 kHz) of this co-doped laser material. This ~100-fold increase in locking bandwidth was achieved via an aggressive lead circuit in the PID controller. The repetition rate can be tuned by controlling the temperature and compressing the CaF_2 spacer via a piezoelectric transducer. The fractional repetition-rate tuning was measured to be ~10^{-5}/K and strain-based tuning was 5×10^{-5}/Mpa when pressure was applied perpendicular to the beam propagation. A fractional tuning range of >10^{-4} was achieved for a 10 K temperature change of the CaF_2 cavity. However, thermal fluctuations in the cavity due to the temperature difference between the cavity and its environment are the limiting factor for long-term repetition-rate stability. Repetition-rate locking will be explored in a future study. Apart from temperature-induced repetition-rate changes, this monolithic design is very resilient to environmental perturbations. Neither acoustic noise nor vibrations had a measurable effect on the offset frequency.

In summary, we have demonstrated, to the best of our knowledge, the first phase-stabilized, fully monolithic solid-state oscillator with a 1 GHz fundamental repetition rate. Despite its much smaller overall size and low power consumption, the favorable parameter regime enables excellent phase-noise performance even at high repetition rates. This level of performance can be achieved in rough environments and rivals even the best gigahertz-repetition-rate Ti:sapphire laser-based frequency combs in terms of amplitude and phase noise. Furthermore, the simple monolithic design of the cavity eliminates the need for tuning and provides a foundation for a portable ultra-low-noise mode-locked laser. With appropriate dispersion compensation, this laser concept could be adapted to generate other wavelengths, pulse durations, and output powers. This new approach is suitable for compact, power-efficient, space-qualified combs and might find applications in
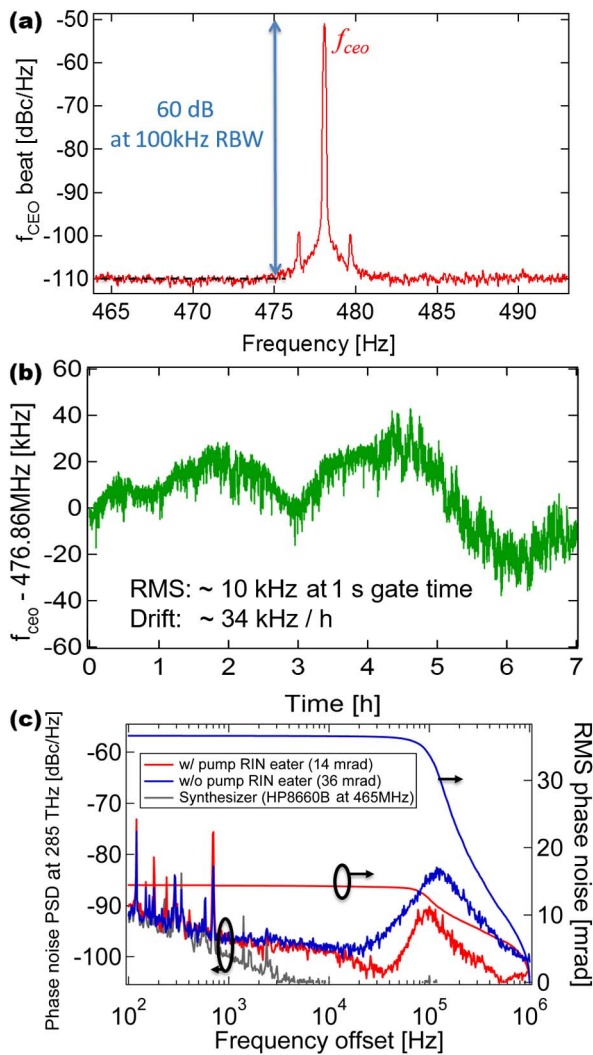
Fig. 4. (a) Free-running f_{ceo} beat note at 100 kHz RBW and averaged over 100 traces. The pronounced sidebands are due to soliton-continuum interaction [30], showing a <9 mrad nonlinear phase shift per round-trip. (b) Free-running f_{ceo} jitter of the monolithic laser over 7 h of continuous operation. (c) Residual single-sided phase-noise power spectral density (PSD) of f_{ceo} when locked to an electronic synthesizer at 465 MHz. Below 1 kHz, the residual PSD, including spurs, was limited by the synthesizer.

instrumentation, precision measurements, and fundamental science.

See Supplement 1 for supporting content.

REFERENCES

1. W. Hänsel, M. Giunta, K. Beha, M. Lezius, M. Fischer, and R. Holzwarth, in *Advanced Solid State Lasers*, OSA Technical Digest (Optical Society of America, 2015), paper ATh4A.2.
2. N. Kuse, J. Jiang, C.-C. Lee, T. R. Schibli, and M. E. Fermann, Opt. Express **24**, 3095 (2016).
3. H. Kim, P. Qin, Y. Song, H. Yang, J. Shin, C. Kim, K. Jung, C. Wang, and J. Kim, IEEE J. Sel. Top. Quantum Electron. **20**, 901108 (2014).
4. R. Paschotta, Appl. Phys. B **79**, 163 (2004).
5. A. Bartels, S. A. Diddams, C. W. Oates, G. Wilpers, J. C. Bergquist, W. H. Oskay, and L. Hollberg, Opt. Lett. **30**, 667 (2005).
6. J. J. McFerran, E. N. Ivanov, A. Bartels, G. Wilpers, C. W. Oates, S. A. Diddams, and L. Hollberg, Electron. Lett. **41**, 650 (2005).
7. J. Millo, M. Abgrall, M. Lours, E. M. L. English, H. Jiang, J. Guéna, A. Clairon, S. Bize, Y. Le Coq, and G. Santarelli, Appl. Phys. Lett. **94**, 141105 (2009).
8. W. Zhang, Z. Xu, M. Lours, R. Boudot, Y. Kersale, G. Sanatarelli, and Y. Le Coq, Appl. Phys. Lett. **96**, 211105 (2010).
9. T. M. Fortier, M. S. Kirchner, F. Quinlan, J. Taylor, J. C. Bergquist, T. Rosenband, N. Lemke, A. Ludlow, Y. Jiang, C. W. Oates, and S. A. Diddams, Nat. Photonics **5**, 425 (2011).
10. W. Sun, F. Quinlan, T. M. Fortier, J. D. Deschenes, Y. Fu, S. A. Diddams, and J. C. Campbell, Phys. Rev. Lett. **113**, 203901 (2014).
11. F. Quinlan, F. N. Baynes, T. M. Fortier, Q. Zhou, A. Cross, J. C. Campbell, and S. A. Diddams, Opt. Lett. **39**, 1581 (2014).
12. J. Kim, K. Jung, J. Shin, C. Jeon, and D. Kwon, J. Lightwave Technol. (2016, to be published).
13. H. Byun, D. Pudo, S. Frolov, A. Hanjani, J. Shmulovich, E. P. Ippen, and F. X. Kärtner, IEEE Photon. Technol. Lett. **21**, 763 (2009).
14. A. Choudhary, A. A. Lagatsky, P. Kannan, W. Sibbett, C. T. A. Brown, and D. P. Shepherd, Opt. Lett. **37**, 4416 (2012).
15. R. Mary, G. Brown, S. J. Beecher, F. Torrisi, S. Milana, D. Popa, T. Hasan, Z. Sun, E. Lidorikis, S. Ohara, A. C. Ferrari, and A. K. Kar, Opt. Express **21**, 7943 (2013).
16. A. A. Lagatsky, A. Choudhary, P. Kannan, D. P. Shepherd, W. Sibbett, and C. T. A. Brown, Opt. Express **21**, 19608 (2013).
17. L. A. Jiang, M. E. Grein, E. P. Ippen, C. McNeilage, J. Searls, and H. Yokoyama, Opt. Lett. **27**, 49 (2002).
18. J. J. Plant, J. T. Gopinath, B. Chann, D. J. Ripin, R. K. Huang, and P. W. Juodawlkis, Opt. Lett. **31**, 223 (2006).
19. M. G. Thompson, A. R. Rae, M. Xia, R. V. Penty, and I. H. White, IEEE J. Sel. Top. Quantum Electron. **15**, 661 (2009).
20. A. R. Criado, C. de Dios, P. Acedo, G. Carpintero, and K. Yvind, J. Lightwave Technol. **30**, 3133 (2012).
21. T. J. Kippenberg, R. Holzwarth, and S. A. Diddams, Science **332**, 555 (2011).
22. P. Del'Haye, T. Herr, E. Gavartin, R. Holzwarth, and T. J. Kippenberg, Phys. Rev. Lett. **107**, 063901 (2011).
23. J. D. Jost, T. Herr, C. Lecaplain, V. Brasch, M. H. P. Pfeiffer, and T. J. Kippenberg, Optica **2**, 706 (2015).
24. X. Yi, Q.-F. Yang, K. Y. Yang, M.-G. Suh, and K. Vahala, Optica **2**, 1078 (2015).
25. W. Liang, D. Eliyahu, V. S. Ilchenko, A. A. Savchenkov, A. B. Matsko, D. Seidel, and L. Maleki, Nat. Commun. **6**, 7957 (2015).
26. T. J. Kane and R. L. Byer, Opt. Lett. **10**, 65 (1985).
27. F. Gires and P. Tournois, C. R. Acad. Sci. Paris **258**, 6112 (1964).
28. U. Keller, K. J. Weingarten, F. X. Kärtner, D. Kopf, B. Braun, I. D. Jung, R. Fluck, C. Hönninger, N. Matuschek, and J. A. der Au, IEEE J. Sel. Top. Quantum Electron. **2**, 435 (1996).
29. C.-C. Lee, Y. Hayashi, K. L. Silverman, A. Feldman, T. Harvey, R. P. Mirin, and T. R. Schibli, Opt. Express **23**, 33038 (2015).
30. C.-C. Lee and T. R. Schibli, Phys. Rev. Lett. **112**, 223903 (2014).